Xanthene-Bridged Cofacial Bisporphyrins

Christopher J. Chang,[†] Yongqi Deng,[†] Alan F. Heyduk,[†] C. K. Chang,*[,‡] and Daniel G. Nocera*[,†]

Departments of Chemistry, Massachusetts Institute of Technology, 77 Massachusetts Avenue, Cambridge, Massachusetts 02139, and Michigan State University, East Lansing, Michigan 48824

Received August 16, 1999

The synthesis and characterization of cofacial bisporphyrins juxtaposed by xanthene-bridged pillars are presented. The one-pot preparation of the xanthene dialdehyde avoids the lengthy bridge synthesis accompanying other cofacial porphyrin systems, thus allowing for the facile preparation of homobimetallic zinc (**10**), copper (**11**), and nickel (**12**) complexes. The cofacial orientation of the two porphyrin macrocycles was confirmed by X-ray crystallography. Structural data are provided for bisporphyrins **10**−**12**: **10** ($C_{79}H_{82}N_8OZn_2$), triclinic, space group $P\bar{1}$, $a = 11.2671(2)$ Å, $b = 14.9809(2)$ Å, $c = 20.4852(2)$ Å, $\alpha = 101.6680(10)°$, $\beta = 100.8890(10)°$, $\gamma = 101.8060(10)°$, $Z = 2$; **11** ($C_{79}H_{82}N_8OCu_2$), triclinic, space group $P\bar{1}$, $a = 11.21410(10)$ Å, $b = 14.9539(5)$ Å, $c = 20.6915(7)$ Å, $\alpha = 101.810(2)°$, $\beta = 101.044(2)°$, $\gamma = 101.722(2)°$, $Z = 2$; **12** ($C_{79}H_{82}N_8ONi_2$), monoclinic, space group $C2/c$, $a = 24.1671(4)$ Å, $b = 10.669$ Å, $c = 50.5080(9)$ Å, $\beta = 99.553(2)°$, $Z = 8$. Exciton interactions between the porphyrin rings are apparent in electronic spectra, consistent with the cofacial superstructure. The combination of structural and spectroscopic data provides a basis for the design of additional metal derivatives for the activation of dioxygen and other small molecules.

Introduction

Cofacial bisporphyrins form molecular clefts for the binding and activation of oxygen and other small molecules. Working in concert, facially disposed subunits can provide the oxidizing or reducing equivalents to effect the overall multielectron activation of small-molecule substrates.[1,2] The majority of cofacial bisporphyrins reported thus far can be grouped into one of two classes: bisporphyrins linked by two or more flexible strapping units[2−21] and pillared bisporphyrins anchored by a single rigid bridge.[1,22−50] Though limited to only two different spacers, anthracene **1** (M_2(DPA)) and biphenylene **2** (M_2(DPB)),[50,51] the pillared systems have been prominent electro-

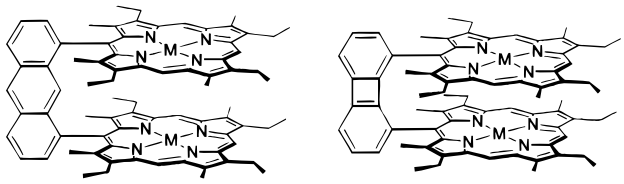

1 **2**

catalysts for the reduction of a variety of small molecules (e.g., O_2, N_2, and H_2).[1,23,24,36,39,52−54] The exceptional activity of **1** and **2**, as compared to their strapped counterparts, derives from the cofacial presentation of the two porphyrin rings with small lateral shifts, while the single bridge allows for a greater range of possible binding geometries within the cofacial pocket by distortion of the porphyrin "bite".

[†] Massachusetts Institute of Technology.
[‡] Michigan State University.

(1) Collman, J. P.; Wagenknecht, P. S.; Hutchinson, J. E. *Angew. Chem., Int. Ed. Engl.* **1994**, *33*, 1537−1554.
(2) Collman, J. P.; Elliot, C. M.; Halbert, T. R.; Tovrog, B. S. *Proc. Natl. Acad. Sci. U.S.A.* **1977**, *74*, 18−22.
(3) Chang, C. K.; Kuo, M. S.; Wang, C. B. *J. Heterocycl. Chem.* **1977**, *14*, 943−945.
(4) Chang, C. K. *J. Heterocycl. Chem.* **1977**, *14*, 1285−1288.
(5) Chang, C. K. *J. Chem. Soc., Chem. Commun.* **1977**, 800−801.
(6) Collman, J. P.; Chong, A. O.; Jameson, G. B.; Oakley, R. T.; Rose, E.; Schmittou, E. R.; Ibers, J. A. *J. Am. Chem. Soc.* **1981**, *103*, 516−533.
(7) Collman, J. P.; Anson, F. C.; Barnes, C. E.; Bencosme, C. S.; Geiger, T.; Evitt, E. R.; Kreh, R. P.; Meier, K.; Pettman, R. B. *J. Am. Chem. Soc.* **1983**, *105*, 2694−2699.
(8) Collman, J. P.; Bencosme, C. S.; Durand Jr., R. R.; Kreh, R. P.; Anson, F. C. *J. Am. Chem. Soc.* **1983**, *105*, 2699−2703.
(9) Collman, J. P.; Bencosme, C. S.; Barnes, C. E.; Miller, B. D. *J. Am. Chem. Soc.* **1983**, *105*, 2704−2710.
(10) Kim, K.; Collman, J. P.; Ibers, J. A. *J. Am. Chem. Soc.* **1988**, *110*, 4242−4246.
(11) Cowan, J. A.; Sanders, J. K. M. *J. Chem. Soc., Chem. Commun.* **1985**, 1213−1214.
(12) Ichimura, K. *Chem. Lett.* **1977**, 641−644.
(13) Kagan, N. E.; Mauzerall, D.; Merrifield, R. B. *J. Am. Chem. Soc.* **1977**, *99*, 5484−5486.
(14) Karaman, R.; Bruice, T. C. *J. Org. Chem.* **1991**, *56*, 3470−3472.
(15) Karaman, R.; Blasko, A.; Almarsson, O.; Arasasingham, R.; Bruice, T. C. *J. Am. Chem. Soc.* **1992**, *114*, 4889−4998.
(16) Karaman, R.; Jeon, S. W.; Almarsson, O.; Bruice, T. C. *J. Am. Chem. Soc.* **1992**, *114*, 4899−4905.
(17) Karaman, R.; Almarsson, O.; Blasko, A.; Bruice, T. C. *J. Org. Chem.* **1992**, *57*, 2169−2173.
(18) Karaman, R.; Almarsson, O.; Bruice, T. C. *J. Org. Chem.* **1992**, *57*, 1555−1559.
(19) Bookser, B. C.; Bruice, T. C. *J. Am. Chem. Soc.* **1991**, *113*, 4208−4218.
(20) Ogoshi, H.; Sugimoto, H.; Yoshida, Z. *Tetrahedron Lett.* **1977**, 169−172.
(21) Paine, J. B., III; Dolphin, D.; Gouterman, M. *Can. J. Chem.* **1978**, *56*, 1712−1715.
(22) Chang, C. K.; Abdalalmuhdi, I. *J. Org. Chem.* **1983**, *48*, 5388−5390.
(23) Chang, C. K.; Liu, H. Y.; Abdalmuhdi, I. *J. Am. Chem. Soc.* **1984**, *106*, 2725−2726.
(24) Chang, C. K.; Abdalmuhdi, I. *Angew. Chem., Int. Ed. Engl.* **1984**, *23*, 164−165.
(25) Fillers, J. P.; Ravichandran, K. G.; Abdalmuhdi, I.; Tulinsky, A.; Chang, C. K. *J. Am. Chem. Soc.* **1986**, *108*, 417−424.
(26) Proniewicz, L. M.; Odo, J.; Goral, J.; Chang, C. K.; Nakamoto, K. *J. Am. Chem. Soc.* **1989**, *111*, 2105−2110.

10.1021/ic990987+ CCC: $19.00
Published on Web 02/10/2000

Owing to our interest in proton-coupled redox processes of small molecules,[55] especially oxygen, we sought to develop methods for the facile assembly of new cofacial bisporphyrins that exhibit variable pocket sizes with minimal lateral displacements. Inspired by Rebek's elegant work on molecular clefts,[56−60] we turned our attention to xanthene[61,62] as a new spacer for cofacial bisporphyrins. We now report that this spacer provides a convenient entry to the construction of a novel "Pac-Man" bisporphyrin that affords a unique combination of chemical stability, rigidity, and synthetic availability. We extend the utility of this cofacial system by also preparing and characterizing the homobinuclear zinc, copper, and nickel complexes.

Experimental Section

Materials. Silica gel 60 (70−230 and 230−400 mesh, Merck) was used for column chromatography. Analytical thin-layer chromatography was performed using Merck 60 F254 silica gel (precoated sheets, 0.2 mm thick). Solvents for the syntheses were of reagent grade or better and were dried according to standard methods.[63] Spectroscopic experiments employed dichloromethane (spectroscopic grade, Burdick & Jackson), which was stored over 4 Å molecular sieves under high vacuum or in a glovebox. Starting materials for the syntheses were obtained as follows: 9,9-dimethylxanthene (**3**) was obtained from xanthone as described by Rebek and co-workers;[56] 2-(ethyloxycarbonyl)-3-ethyl-4-methylpyrrole (**4**) was prepared from ethyl isocyanoacetate[64] and 3-acetoxy-2-nitropentane[65,66] by the method of Barton and Zard;[67] and bis(3-ethyl-5-formyl-4-methyl-2-pyrryl)methane (**5**) was synthesized by following literature procedures.[68−72] All other reagents were used as received. Mass spectral analyses were carried out by the University of Illinois Mass Spectrometry Laboratory. Elemental analyses were performed at H. Kolbe Mikroanalytisches Laboratorium.

4,5-Diformyl-9,9-dimethylxanthene (6). *n*-Butyllithium (1.6 M in hexanes, 134 mL, 0.214 mol, 3 equiv) was added to **3** (15 g, 0.071 mol) dissolved in 80 mL of dry hexane containing *N*,*N*,*N*′,*N*′-tetramethylethylenediamine (27 mL, 0.178 mol, 2.5 equiv). The mixture was refluxed under nitrogen for 10 min and cooled to 0 °C, after which 30 mL of DMF was added. The stirred mixture was allowed to warm slowly to room temperature over a period of 2 h and then poured over ice. The precipitate was collected by filtration and recrystallized from hot methanol to afford **6** as an off-white solid (16.2 g, 86% yield). ^{1}H NMR (300 MHz, $CDCl_3$, 25 °C): δ = 10.68 (s, 2H, CHO), 7.82 (d, 2H, Ar H), 7.75 (d, 2H, Ar H), 7.25 (t, 2H, Ar H), 1.69 (s, 6H, CH_3).

4,5-Bis[bis(ethyloxycarbonyl)-4-ethyl-3-methyl-2-pyrryl)methyl]-9,9-dimethylxanthene (7). A mixture of **6** (2.66 g, 0.01 mol) and **4** (7.60 g, 0.042 mol) in absolute ethanol (65 mL) containing concentrated HCl (1.8 mL) was refluxed under nitrogen for 4 h and cooled in an ice−water bath. The precipitate was filtered off and washed with cold methanol to give **7** as a pale-pink powder (8.4 g, 88% yield). ^{1}H NMR (300 MHz, $CDCl_3$, 25 °C): δ = 8.19 (br s, 4H, NH), 7.40 (d, 2H, Ar H), 7.03 (t, 2H, Ar H), 6.67 (d, 2H, Ar H), 5.59 (s, 2H, CH), 4.21 (q, 8H, CH_2), 2.67 (q, 8H, CH_2), 1.66 (s, 6H, CH_3), 1.55 (s, 12H, CH_3), 1.26 (t, 12H, CH_3), 1.04 (t, 12H, CH_3).

4,5-Bis[bis(4-ethyl-3-methyl-2-pyrryl)methyl]-9,9-dimethylxanthene (8). Powdered NaOH (2 g) and **7** (4.2 g, 4.40 mmol) were suspended in 40 mL of ethylene glycol, and the mixture was refluxed under nitrogen for 4 h. The precipitate was collected by suction filtration, washed with water until the washings became neutral, and dried under vacuum over P_2O_5. Product **8**, which was obtained as a goldenrod solid (2.52 g, 86% yield), was stored under nitrogen at −20 °C. ^{1}H NMR (300 MHz, $CDCl_3$, 25 °C): δ = 7.38 (d, 4H, Ar H), 7.03

(27) Collman, J. P.; Kim, K.; Garner, J. M. *J. Chem. Soc., Chem. Commun.* **1986**, 1711−1713.
(28) Collman, J. P.; Kim, K.; Leidner, C. R. *Inorg. Chem.* **1987**, *26*, 1152−1157.
(29) Collman, J. P.; Hutchinson, J. E.; Lopez, M. A.; Tabard, A.; Guilard, R.; Seok, W. K.; Ibers, J. A.; L'Her, M. *J. Am. Chem. Soc.* **1992**, *114*, 9869−9877.
(30) Collman, J. P.; Hutchinson, J. E.; Lopez, M. A.; Guilard, R. *J. Am. Chem. Soc.* **1992**, *114*, 8066−8073.
(31) Collman, J. P.; Hutchinson, J. E.; Ennis, M. S.; Lopez, M. A.; Guilard, R. *J. Am. Chem. Soc.* **1992**, *114*, 8074−8080.
(32) Collman, J. P.; Ha, Y.; Wagenknecht, P. S.; Lopez, M. A.; Guilard, R. *J. Am. Chem. Soc.* **1993**, *115*, 9080−9088.
(33) Collman, J. P.; Ha, Y. Y.; Guilard, R.; Lopez, M. A. *Inorg. Chem.* **1993**, *32*, 1788−1794.
(34) Guilard, R.; Lopez, M. A.; Tabard, A.; Richard, P.; Lecomte, C.; Brandes, S.; Hutchinson, J. E.; Collman, J. P. *J. Am. Chem. Soc.* **1992**, *114*, 9877−9889.
(35) Guilard, R.; Brandes, S.; Tabard, A.; Bouhmaida, N.; LeComte, C.; Richard, P.; Latour, J. M. *J. Am. Chem. Soc.* **1994**, *116*, 10202−10211.
(36) Guilard, R.; Brandes, S.; Tardieux, C.; Tabard, A.; L'Her, M.; Miry, C.; Gouerac, P.; Knop, Y.; Collman, J. P. *J. Am. Chem. Soc.* **1995**, *117*, 11721−11729.
(37) Ichihara, K.; Naruta, Y. *Chem. Lett.* **1998**, 185−186.
(38) Le Mest, Y.; L'Her, M.; Hendricks, N. H.; Kim, K.; Collman, J. P. *Inorg. Chem.* **1992**, *31*, 835−847.
(39) Le Mest, Y.; Inisan, C.; Laouenan, A.; L'Her, M.; Talarmain, J.; El Khalifa, M.; Saillard, J. Y. *J. Am. Chem. Soc.* **1997**, *119*, 6905−6106.
(40) Naruta, Y.; Maruyama, K. *J. Am. Chem. Soc.* **1991**, *113*, 3595−3596.
(41) Naruta, Y.; Sasayama, M.; Maruyama, K. *Chem. Lett.* **1992**, 1267−1270.
(42) Naruta, Y.; Sasayama, M. *J. Chem. Soc., Chem. Commun.* **1994**, 2667−2668.
(43) Naruta, Y.; Sawada, N.; Tadokoro, M. *Chem. Lett.* **1994**, 1713−1716.
(44) Naruta, Y.; Sasayama, M. *Chem. Lett.* **1994**, 2411−2414.
(45) Naruta, Y.; Sasayama, M.; Sasaki, T. *Angew. Chem., Int. Ed. Engl.* **1994**, *33*, 1839−1841.
(46) Naruta, Y.; Sasayama, M.; Ichihara, K. *J. Mol. Catal. A* **1997**, *117*, 115−121.
(47) Chardon-Noblat, S.; Sauvage, J. P.; Mathis, P. *Angew. Chem., Int. Ed. Engl.* **1989**, *28*, 593−595.
(48) Brun, A.; Harriman, A.; Heitz, V.; Sauvage, J. P. *J. Am. Chem. Soc.* **1991**, *113*, 8657−8663.
(49) Harriman, A.; Heitz, V.; Sauvage, J. P. *J. Phys. Chem.* **1993**, *97*, 5940−5946.
(50) Sauvage and co-workers have utilized phenantholine and bipyridine linkers in the assembly of porphyrin-stoppered rotaxane structures as models for the photosynthetic reaction center: Harriman, A.; Sauvage, J. P. *Chem. Soc. Rev.* **1996**, *25*, 41−49.
(51) Smith and co-workers have prepared flexible, singly bridged *cis*-ethene cofacial bisporphyrins that thermally isomerize to their trans counterparts (see refs 83−86).
(52) Ni, C.-L.; Abdalmuhdi, I.; Chang, C. K.; Anson, F. C. *J. Phys. Chem.* **1987**, *91*, 1158−1166.
(53) Lui, H.-Y.; Abdalmuhdi, I.; Chang, C. K.; Anson, F. C. *J. Phys. Chem.* **1985**, *89*, 665−670.
(54) Le Mest, Y.; L'Her, M.; Saillard, J. Y. *Inorg. Chim. Acta* **1996**, *248*, 181−191.
(55) Cukier, R. I.; Nocera, D. G. *Annu. Rev. Phys. Chem.* **1998**, *49*, 337−369.
(56) Nowick, J. S.; Ballester, P.; Ebmeyer, F.; Rebek, J., Jr. *J. Am. Chem. Soc.* **1990**, *112*, 8902−8906.
(57) Hamann, B. C.; Branda, N. R.; Rebek, J., Jr. *Tetrahedron Lett.* **1995**, *34*, 6837−6840.
(58) Park, T. K.; Feng, Q.; Rebek, J., Jr. *J. Am. Chem. Soc.* **1992**, *114*, 4529−4532.
(59) Shimizu, K. D.; Rebek, J., Jr. *Proc. Natl. Acad. Sci U.S.A.* **1996**, *93*, 4257−4260.
(60) Shimizu, K. D.; Dewey, T. M.; Rebek, J., Jr. *J. Am. Chem. Soc.* **1994**, *116*, 5145−5149.
(61) Shipps, G.; Rebek, J., Jr. *Tetrahedron Lett.* **1994**, *35*, 6823−6825.
(62) Shinoda, S.; Tsukube, H.; Nishimura, Y.; Yamazaki, I.; Osuka, A. *J. Org. Chem.* **1969**, *34*, 3757−3762.
(63) Armarego, W. L. F.; Perrin, D. D. *Purification of Laboratory Chemicals*, 4th ed.; Butterworth-Heinmann: Oxford, U.K., 1996.
(64) Harman, G. D.; Wenstock, L. M. *Organic Syntheses*; Wiley: New York, 1988; Collect. Vol. VI, pp 620−624.
(65) Sprang, C. A.; Egering, E. F. *J. Am. Chem. Soc.* **1942**, *64*, 1063−1064.
(66) Tindall, J. B. *Ind. Eng. Chem.* **1941**, *33*, 65−66.
(67) Barton, D. H. R.; Zard, S. Z. *J. Chem. Soc., Chem. Commun.* **1985**, 1098−1100.
(68) Johnson, A. W.; Markham, E.; Price, R.; Shaw, K. B. *J. Chem. Soc.* **1959**, 4251−4257.
(69) Johnson, A. W.; Kay, I. T.; Markham, E.; Price, R.; Shaw, K. B. *J. Chem. Soc.* **1959**, 3416−3424.
(70) Kleinspehn, G. G. *J. Am. Chem. Soc.* **1955**, *77*, 1546−1548.
(71) Abraham, R. J.; Jackson, A. H.; Kenner, G. W.; Warburton, D. *J. Chem. Soc.* **1963**, 853−862.
(72) Chong, R.; Clezy, P. S.; Liepa, A. J.; Nichol, A. W. *Aust. J. Chem.* **1969**, *22*, 229−238.

(t, 2H, Ar H), 6.81 (br s, 2H, CH), 6.29 (s, 4H, NH), 5.68 (br s, 2H, CH), 2.38 (q, 8H, CH_2), 1.62 (s, 18H, CH_3), 1.13 (t, 12H, CH_3).

4,5-Bis[(2,3,13,17-tetraethyl-3,7,12,18-tetramethyl-5-porphyrinyl)-9,9-dimethylxanthene, H_4(DPX) (9). A suspension of **8** (5.30 g, 8 mmol) and **5** (4.58 g, 16 mmol) in a mixture of THF (800 mL) and methanol (400 mL) was purged with nitrogen for 1 h. A solution of *p*-toluenesulfonic acid (3.56 g) in methanol (20 mL) was added dropwise over a period of 2 h. The resulting red mixture was stirred in the dark under nitrogen for 2 days. Solid *o*-chloranil (3.56 g) was added in one portion, and stirring was continued in air for 24 h. The mixture was taken to dryness and the remaining solid redissolved in 500 mL of chloroform. A saturated methanolic solution of $Zn(OAc)_2 \cdot 2H_2O$ (25 mL) was added, and the solution was refluxed for 15 min. The solvent was removed, and the remaining residue was purified by flash column chromatography (silica gel, dichloromethane). The first band eluted was collected and vigorously stirred with 6 N HCl (15 mL) for 15 min. The solution was neutralized with a 10% aqueous sodium carbonate solution, and the mixture was stirred for an additional 15 min. The organic phase was separated from the mixture, washed with water (3 × 50 mL), dried over Na_2SO_4, and taken to dryness. Purification by flash column chromatography (silica gel, dichloromethane to 1:1 methanol/dichloromethane) followed by recrystallization from dichloromethane/methanol afforded pure **9** as a purple microcrystalline powder (2.1 g, 23% yield). ^{1}H NMR (300 MHz, $CDCl_3$, 25 °C): δ = 9.13 (s, 2H, meso), 8.29 (s, 4H, meso), 7.88 (d, 2H, Ar H), 7.28 (t, 2H, Ar H), 7.06 (d, 2H, Ar H), 4.12 (m, 4H, CH_2), 3.86 (m, 4H, CH_2), 3.32 (m, 8H, CH_2), 3.10 (s, 12H, CH_3), 2.29 (s, 12H, CH_3), 2.25 (s, 6H, CH_3), 1.75 (t, 12H, CH_3), 1.37 (t, 12H, CH_3), −6.42 (br s, 2H, NH), −6.80 (br s, 2H, NH).

Zn_2(DPX) (10). A saturated methanolic solution of $Zn(OAc)_2 \cdot 2H_2O$ (1 mL) was added to a solution of **9** (20 mg, 0.017 mmol) in 5 mL of chloroform. The reaction mixture was refluxed for 30 min and taken to dryness. The solid residue was purified by flash column chromatography (silica gel, 3:1 dichloromethane/hexanes) followed by recrystallization from dichloromethane/methanol to yield analytically pure **10** as a brick red solid in nearly essentially quantitative yield. ^{1}H NMR (300 MHz, $CDCl_3$, 25 °C): δ = 9.13 (s, 2H, meso), 8.43 (s, 4H, meso), 7.85 (d, 2H, Ar H), 7.21 (t, 2H, Ar H), 6.95 (d, 2H, Ar H), 4.15 (m, 4H, CH_2), 3.87 (m, 4H, CH_2), 3.56 (m, 4H, CH_2), 3.32 (m, 4H, CH_2), 3.21 (s, 12H, CH_3), 2.29 (s, 12H, CH_3), 2.24 (s, 6H, CH_3), 1.74 (t, 12H, CH_3), 1.40 (t, 12H, CH_3). Anal. Calcd for $C_{79}H_{82}N_8OZn_2$: C, 73.54; H, 6.41; N, 8.68. Found: C, 73.69; H, 6.15; N, 8.35. HRFABMS (M^+), *m*/*z*: calcd for $C_{79}H_{82}N_8OZn_2$, 1286.519; found, 1286.520.

Cu_2(DPX) (11). To a 60 mL chloroform solution of **9** (90 mg, 0.077 mmol) was added a solution of $Cu(OAc)_2 \cdot 2H_2O$ (200 mg) and potassium acetate (200 mg) in 15 mL of methanol. The resulting solution was refluxed for 4 h, and the solvent was removed by rotary evaporation. The solid was taken up in a 1:1 mixture of dichloromethane/water (120 mL). The organic layer was decanted, washed with water (3 × 50 mL), dried over Na_2SO_4, and taken to dryness. The crude material was purified by flash column chromatography (silica gel, 1:1 dichloromethane/hexanes) followed by recrystallization from dichloromethane/methanol to afford analytically pure **11** as a mulberry red solid (94 mg, 94% yield). Anal. Calcd for $C_{79}H_{82}N_8OCu_2 \cdot 2CH_2Cl_2$: C, 66.85; H, 5.91; N, 7.70. Found: C, 67.25; H, 5.95; N, 7.41. HRFABMS (M^+), *m*/*z*: calcd for $C_{79}H_{82}N_8OCu_2$, 1284.540; found, 1284.519.

Ni_2(DPX) (12). A mixture of **9** (88 mg, 0.076 mmol) and $NiCl_2$ (123 mg) in 50 mL of DMF was refluxed under nitrogen for 4 h. The solvent was removed under vacuum, and the remaining solid was taken up in a 1:1 mixture of dichloromethane/water (150 mL). The organic layer was decanted, washed with water (3 × 50 mL), dried over Na_2SO_4, and taken to dryness. Purification by flash column chromatography (silica gel, 3:1 dichloromethane/hexanes) followed by recrystallization from dichloromethane/methanol gave analytically pure **12** as a plum red solid (80 mg, 83% yield). ^{1}H NMR (300 MHz, $CDCl_3$, 25 °C): δ = 8.76 (s, 2H, meso), 8.00 (s, 4H, meso), 7.79 (d, 2H, Ar H), 7.19 (t, 2H, Ar H), 6.93 (d, 2H, Ar H), 3.64 (m, 4H, CH_2), 3.47 (m, 4H, CH_2), 2.95 (m, 8H, CH_2), 2.71 (s, 12H, CH_3), 2.12 (s, 12H, CH_3), 1.57 (t, 12H, CH_3), 1.52 (s, 6H, CH_3), 1.22 (t, 12H, CH_3). Anal. Calcd for $C_{79}H_{82}N_8ONi_2 \cdot 3H_2O$: C, 71.29; H, 6.61; N, 8.42. Found: C, 71.01; H, 6.65; N, 8.25. HRFABMS (M^+) *m*/*z*: calcd for $C_{79}H_{82}N_8ONi_2$, 1274.532; found, 1274.531.

General Details of X-ray Data Collection and Reduction. X-ray diffraction data were collected using a Siemens three-circle diffractometer equipped with a CCD detector. Measurements were carried out at −90 °C using Mo Kα (λ = 0.71073 Å) radiation, which was wavelength-selected with a single-crystal graphite monochromator. Four sets of data were collected using ω scans and a −0.3° scan width. All calculations were performed using a Silicon Graphics Indigo 2 workstation. The data frames were integrated to *hkl*/intensity, and final unit cells were calculated by using the SAINT v.4.050 program from Siemens. The structures were solved and refined with the SHELXTL v.5.03 suite of programs developed by G. M. Sheldrick and Siemens Industrial Automation, Inc., 1995. Plots were drawn using ORTEP.[73]

X-ray Structure of Zn_2(DPX) (10). A 0.2 mm × 0.2 mm × 0.08 mm deep brick red crystal of plate morphology was obtained from a solution of the complex in a mixture of methanol and dichloromethane. The crystal was coated with Paratone N and mounted onto a glass fiber. A total of 13 185 reflections were collected in the θ range 1.43−23.28°, of which 8982 were unique (R_{int} = 0.0300). The zinc atoms were located by the Patterson method, and remaining atoms were located by standard difference Fourier techniques. Hydrogen atoms were placed in calculated positions using a standard riding model and were refined isotropically. A disordered ethyl group attached to C(33) was assigned half-occupancy in two different conformations. The largest peak and hole in the difference map were 0.671 and −0.534 e Å^{-3}, respectively. The least-squares refinement converged normally giving residuals of R1 = 0.0570 and wR2 = 0.1559, with GOF = 1.116. Crystal data for $C_{79}H_{77}N_8OZn_2$: triclinic, $P\bar{1}$, Z = 2, a = 11.2671(2) Å, b = 14.9809(2) Å, c = 20.4852(2) Å, α = 101.6680(10)°, β = 100.8890(10)°, γ = 101.8060(10)°, V = 3217.57(8) Å^3, ρ_{calc} = 1.327 g/cm^3, F(000) = 1350.

X-ray Structure of Cu_2(DPX) (11). A 0.3 mm × 0.2 mm × 0.08 mm mulberry red crystal of plate morphology was obtained from a solution of the complex in a mixture of methanol and dichloromethane. The crystal was coated with Paratone N and mounted onto a glass fiber. A total of 11 372 reflections were collected in the θ range 1.54−21.50°, of which 7353 were unique (R_{int} = 0.1015). The copper atoms were located by the Patterson method, and the remaining atoms in the structure were located as peaks in the difference Fourier map. Hydrogen atoms were placed in calculated positions using a standard riding model and were refined isotropically. The largest peak and hole in the difference map were 0.788 and −0.629 e Å^{-3}, respectively. The least-squares refinement converged normally giving residuals of R1 = 0.0909 and wR2 = 0.1994, with GOF = 1.036. Crystal data for $C_{79}H_{82}Cu_2N_8O$: triclinic, $P\bar{1}$, Z = 2, a = 11.21410(10) Å, b = 14.9539(5) Å, c = 20.6915(7) Å, α = 101.810(2)°, β = 101.044(2)°, γ = 101.722(2)°, V = 3225.7(2) Å^3, ρ_{calc} = 1.325 g/cm^3, F(000) = 1356.

X-ray Structure of Ni_2(DPX) (12). A 0.2 mm × 0.15 mm × 0.08 mm plum red crystal of plate morphology was obtained from a solution of the complex in a mixture of methanol and dichloromethane. The crystal was coated with Paratone N and mounted onto a glass fiber. A total of 18 577 reflections were collected in the θ range 1.64−20.00°, of which 5996 were unique (R_{int} = 0.1005). The Patterson method was used to locate the nickel atoms, all remaining atoms were placed using the difference Fourier map. Hydrogen atoms were placed in calculated positions using a standard riding model and were refined isotropically. The largest peak and hole in the difference map were 0.509 and −0.425 e Å^{-3}, respectively. The least-squares refinement converged normally giving residuals of R1 = 0.0768 and wR2 = 0.1460, with GOF = 1.173. Crystal data for $C_{79}H_{82}N_8Ni_2O$: monoclinic, $C2/c$, Z = 8, a = 24.1671(4) Å, b = 10.669(0) Å, c = 50.5080(9) Å, β = 99.553(2)°, V = 12842.0(3) Å^3, ρ_{calc} = 1.321 g/cm^3, F(000) = 5408.

Physical Measurements. ^{1}H NMR spectra were collected in $CDCl_3$ (Cambridge Isotope Laboratories) at the MIT Department of Chemistry Instrumentation Facility (DCIF) using a Varian XL-300, a Unity 300, or a Mercury 300 spectrometer at 25 °C. All chemical shifts are reported using the standard δ notation in parts per million; positive chemical shifts are to higher frequency from the given reference. Absorption

(73) Johnson, C. K. *ORTEP II*; Report ORNL-5138; Oak Ridge National Laboratory: Oak Ridge, TN, 1976.

Scheme 1[a]

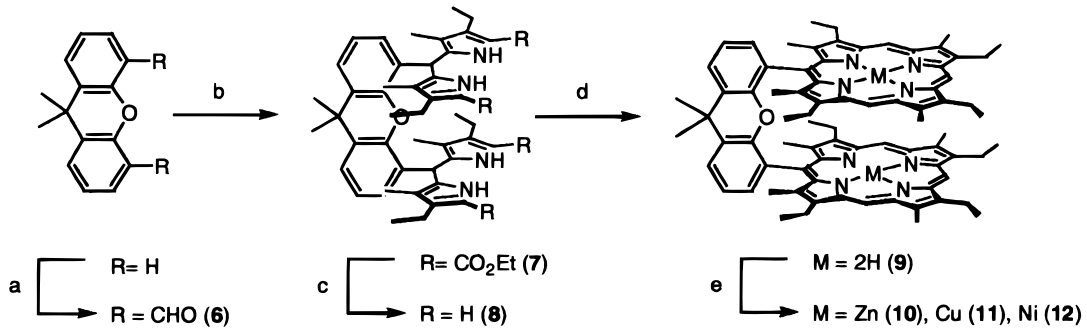

[a] Key: (a) i, *n*-BuLi; ii, DMF; iii, H_2O. (b) **6** and **4**, ethanol, HCl, reflux. (c) NaOH, ethylene glycol, reflux. (d) i, **8** and **5**, *p*-TsOH, methanol/THF; ii, *o*-chloranil. (e) MX_2, chloroform/methanol/DMF, reflux.

spectra were obtained using a Cary 17 spectrophotometer modified by On-Line Instrument Systems (OLIS) to include computer control. Emission spectra were recorded using a high-resolution instrument described previously.[74]

Luminescence lifetime measurements were carried out using a Hamamatsu C4334-0 streak camera. Excitation pulses (95 μJ, 400 nm) were generated from the second harmonic of a commercial 1 kHz Ti:sapphire-based chirped-pulse regenerative amplifier system. Briefly, the amplifier (Alpha 1000 S, BM Industries) was seeded with 130 fs, 30−40 nJ pulses from a 76 MHz passively mode-locked Ti:sapphire oscillator (Mira 900-F, Coherent), pumped by 5 W of second-harmonic light from a solid-state diode pumped YAG laser at 532 nm (Verdi, Coherent). The regenerative amplifier was pumped by 400 ns pulses of 527 nm second-harmonic excitation at 1 kHz from a Nd:YLF laser (BMI 621-D). Chirped pulses from the oscillator were amplified over several passes and compressed in a grating compressor to 100−200 fs pulses at 800 nm with an average power of 800 mW or 0.8 mJ per pulse. Approximately 40% of the light was split off and doubled to 400 nm in a BBO to give 95 mW at 400 nm.

Samples for lifetime measurements were contained within a cell equipped with a solvent resevoir and a 1 cm clear fused-quartz cell (Starna Cells, Inc.). The two chambers were isolated from each other by a high-vacuum Teflon valve and from the environment with a second high-vacuum Teflon valve. Samples were subject to at least three freeze−pump−thaw cycles (10^{-6} Torr).

Magnetic measurements were performed using a SQUID susceptometer (Quantum Design MPMSR2) within the 2−300 K regime. The data were corrected for the diamagnetic contribution of the sample holder and for the diamagnetism of the compound, calculated using Pascal's constants.

Results and Discussion

Synthesis. The xanthene-bridged cofacial bisporphyrin H_4(DPX) (**9**) is synthesized as outlined in Scheme 1. We employ the method originally developed by Chang[22,24] and elaborated by Collman[29] for the preparation of pillared anthracene- and biphenylene-bridged bisporphyrins. This convergent route involves a three-branch coupling of the dicarboxaldehyde bridge **6**, α-free pyrrole ethyl ester **4**, and dipyrrylmethanedialdehyde **5** to form the cofacial bisporphyrin.

Dialdehyde bridge **6** is obtained in 86% yield by the regioselective 4,5-dilithiation of 9,9-dimethylxanthene **3** in the presence of dry DMF followed by hydrolysis of the intermediate imidate salt. Reaction of **6** with 4 equiv of **4** in boiling ethanol affords the corresponding ester-protected bis(pyrryl)methane **7** in 88% yield. Subsequent saponification of the α-ethyl esters of **7** with sodium hydroxide in ethylene glycol proceeds smoothly to produce the α-free tetrapyrrole **8** (86% yield). Cyclization of **8** with **5** in the presence of *p*-toluenesulfonic acid followed by oxidation with *o*-chloranil gives the corresponding bisporphyrin **9** after workup and purification. The 23% yield for the final coupling step is comparable to the results obtained by the optimized procedure employed by Collman and co-workers for the synthesis of H_4(DPB).[29]

The cofacial disposition of rings in bisporphyrin **9** is revealed by ^{1}H NMR spectroscopy. The upfield shift of the internal NH pyrrolic resonances in the ^{1}H NMR spectrum of **9** compared to the signals of its monomeric counterpart[75] is characteristic of a cofacial arrangement, due to a shielding effect caused by ring current interactions between the closely associated porphyrin moieties.[1,22,24] The clean, sharp NMR peaks observed for the meso and methyl protons of **9** provide further support for a nonslipped, stacked conformation for the two adjoined porphyrin rings.

The homobimetallic complexes of bisporphyrin **9** are readily obtained by reaction with metal salts. Treatment of **9** with Zn(OAc)$_2$·2H$_2$O in methanol/chloroform mixtures affords the corresponding binuclear zinc(II) complex Zn_2(DPX) (**10**) in quantitative yield. Complex **10** was identified using a combination of ^{1}H NMR, high-resolution mass spectrometry, and elemental analyses. Similar to that of **9**, the ^{1}H NMR spectrum of **10** confirms a diamagnetic, cofacially stacked bisporphyrin system. The homobimetallic complex Cu_2(DPX) (**11**) is obtained in excellent yield (94%) by reaction of **9** with Cu(OAc)$_2$·2H$_2$O in methanol/chloroform mixtures. Complex **11** gave satisfactory mass spectral and elemental analyses. Magnetic susceptibility measurements over the temperature range 2−300 K verified the paramagnetic nature of **11**. The compound obeys the Curie law at high temperatures with a magnetic moment of 1.72 μ_B per metal center, though deviations from a simple paramagnet are observed at low temperature. A magnetic moment of 1.58 μ_B per metal center at 2 K indicates weak antiferromagnetic coupling. A fit of the molar susceptibility data to the Bleaney−Bowers model for dimers[76] gives an estimate for the exchange coupling constant J of -0.5 cm^{-1}, a value that corresponds to the lower limit value obtained by EPR for a series of cofacial copper bisporphyrins.[77] Lastly, Ni_2(DPX) **(12)** was prepared according to Adler's method ($NiCl_2$/refluxing DMF)[78] in good yield (83%). The diamagnetic complex was characterized by ^{1}H NMR, high-resolution mass spectrometry, and elemental analyses.

(74) Shin, Y.-g. K.; Miskowski, V. M.; Nocera, D. G. *Inorg. Chem.* **1990**, *29*, 2308−2313.

(75) The chemical shifts obtained for the internal NH protons in a monomeric mono(meso-substituted porphyrin) xanthene are δ −3.10 and −3.29 ppm.

(76) Carlin, R. L. *Magnetochemistry*; Springer-Verlag: Berlin, 1986.

(77) Eaton, S. S.; Eaton, G. R.; Chang, C. K. *J. Am. Chem. Soc.* **1985**, *107*, 3177−3184.

(78) Scheidt, W. R.; Mondal, J. U.; Eigenbrot, C. W.; Adler, A.; Radonovich, L. J.; Hoard, J. L. *Inorg. Chem.* **1986**, *25*, 795−799.

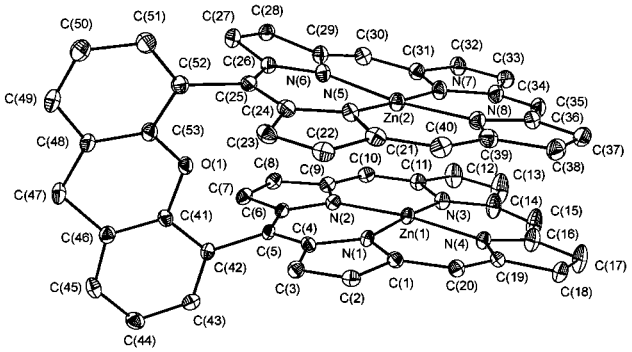

Figure 1. Crystal structure of Zn_2(DPX) (**10**). Thermal ellipsoids are drawn at the 25% probability level, showing the atom-numbering scheme. Side groups and hydrogen atoms have been omitted for clarity.

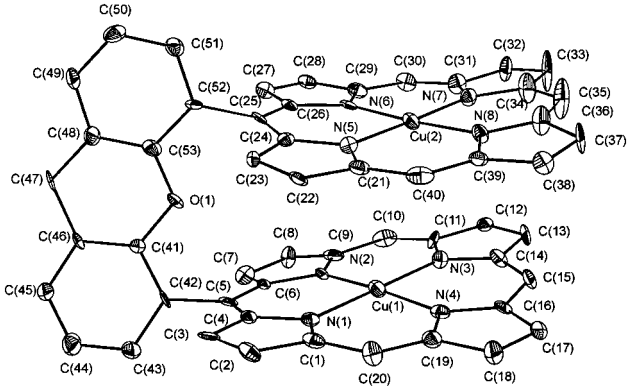

Figure 2. Crystal structure of Cu_2(DPX) (**11**). Thermal ellipsoids are drawn at the 25% probability level, showing the atom-numbering scheme. Side groups and hydrogen atoms have been omitted for clarity.

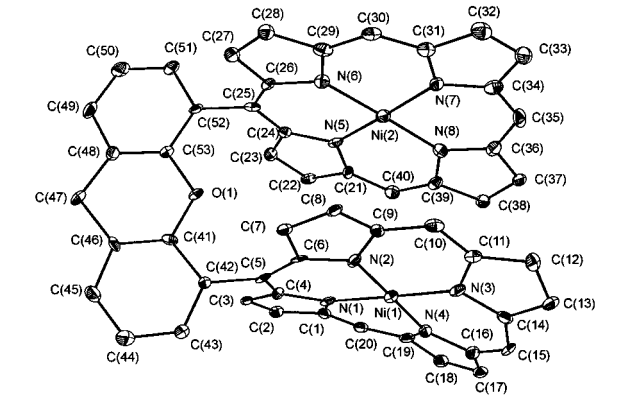

Figure 3. Crystal structure of Ni_2(DPX) (**12**). Thermal ellipsoids are drawn at the 25% probability level, showing the atom-numbering scheme. Side groups and hydrogen atoms have been omitted for clarity.

Structural Chemistry of DPX. The molecular structures of **10**−**12** are shown in Figures 1−3, respectively. Each atom of the porphyrin rings and the corresponding bridge is numbered in the standard fashion while auxiliary methyl and ethyl groups off the macrocycles are additionally identified with their connection to the porphyrin ring. Selected geometrical measurements are given in Tables 1−4.

Trends in bond lengths and angles of macrocyclic core structures and side chains agree well with those observed in related systems such as H_4(DPA), H_4(DPB), and 1,2-bis(2,3,7,8,-12,13,17,18-octaethyl-5-porphyrinyl)-*cis*-ethene porphyrins.[78−80] Structural highlights of the core structures for **10**-**12** are as follows.

10. Both tetracoordinate Zn(II) macrocycles exhibit a wave conformation,[78,79,81] with a mean deviation of 0.3608 Å for the macrocyclic atoms from the porphyrin mean plane. Each macrocycle is positioned essentially in the N_4 plane (average Zn−N_4 displacement = 0.0918 Å) with an average Zn−N bond length of 2.041 Å, which is in good agreement with the cases of related monomeric[79,80] and dimeric Zn(II) porphyrins.[82−84]

Table 1. Crystallographic Data for **10**−**12**

	10	**11**	**12**
empirical formula	$C_{79}H_{77}N_8OZn_2$	$C_{79}H_{82}Cu_2N_8O$	$C_{79}H_{82}N_8Ni_2O$
fw	1285.23	1286.61	1276.95
T (K)	183(2)	183(2)	183(2)
λ (Å)	0.710 73	0.710 73	0.710 73
crystal system	triclinic	triclinic	monoclinic
space group	$P\bar{1}$	$P\bar{1}$	$C2/c$
a (Å)	11.2671(2)	11.21410(10)	24.1671(4)
b (Å)	14.9809(2)	14.9539(5)	10.669
c (Å)	20.4852(2)	20.6915(7)	50.5080(9)
α (deg)	101.6680(10)	101.810(2)	90
β (deg)	100.8890(10)	101.044(2)	99.553(2)
γ (deg)	101.8060(10)	101.722(2)	90
V (Å^3)	3217.57(8)	3225.7(2)	12 842.0(3)
Z	2	2	8
ρ_{calcd} (g cm^{-3})	1.327	1.325	1.321
abs coeff (mm^{-1})	0.800	0.714	0.641
F(000)	1350	1356	5408
no. of reflcns collcd	13 185	11 372	18 577
(R_{int}) ind reflns	8982 (0.0300)	7353 (0.1015)	5996 (0.1005)
max/min transm	0.4175/0.3605	0.4239/0.3066	0.4885/0.3535
data/restraints/params	8972/0/830	6093/0/812	5623/0/812
R1,[a] wR2[b]	0.0570, 0.1559	0.0909, 0.1994	0.0768, 0.1460
R1,[a] wR2[b] (all data)	0.0833, 0.1973	0.1940, 0.2897	0.1152, 0.2051
GOF[c] on F^2	1.116	1.036	1.173
extinction coeff	0.0029(8)	0.0000(3)	0.00000(2)

[a] $R1 = \sum||F_o| - |F_c||/\sum|F_o|$. [b] $wR2 = [\sum w(F_o^2 - F_c^2)^2/\sum w(F_o^2)^2]^{1/2}$. [c] $GOF = [\sum w(F_o^2 - F_c^2)^2/(n - p)]^{1/2}$, where n is the number of data and p is the number of parameters refined.

Table 2. Crystallographically Derived Intradimer Geometrical Features for **10**−**12**[a]

	10	**11**	**12**
M−M dist (Å)	3.708	3.910	4.689
M−N_4 displacement (Å)	0.0918	0.0290	0.0061
Ct−Ct dist (Å)	3.863	3.978	4.698
MPS (Å)	3.417	3.611	3.666
interplanar angle (deg)	4.4	2.3	1.9
slip angle (deg)	27.8	24.8	38.7
lateral shift (Å)	1.802	1.668	2.937

[a] Metrics were derived as follows. The macrocyclic center (Ct) was calculated as the center of the four-nitrogen plane (4-N plane) for each macrocycle. The interplanar angle was measured as the angle between the 4-N least-squares planes. The plane separation was measured as the perpendicular distance from one macrocycle's 4-N least-squares plane to the center of the other macrocycle; the mean plane separation (MPS) was the average of the two plane separations. The slip angle (α) was calculated as the average angle between the vector connecting the two metal centers and the unit vectors normal to the two macrocyclic 4-N least-squares planes ($\alpha = \alpha_1 + \alpha_2/2$). The lateral shift was defined as (sin α)(Ct−Ct dist).

Table 3. Selected Bond Lengths (Å) for **10**−**12**

10		**11**		**12**	
Zn(1)−N(1)	2.031(4)	Cu(1)−N(1)	2.008(9)	Ni(1)−N(1)	1.942(7)
Zn(1)−N(2)	2.036(4)	Cu(1)−N(2)	2.016(9)	Ni(1)−N(2)	1.943(7)
Zn(1)−N(3)	2.040(4)	Cu(1)−N(3)	2.001(9)	Ni(1)−N(3)	1.948(7)
Zn(1)−N(4)	2.051(4)	Cu(1)−N(4)	2.011(9)	Ni(1)−N(4)	1.920(7)
Zn(2)−N(5)	2.047(4)	Cu(2)−N(5)	1.980(10)	Ni(2)−N(5)	1.968(7)
Zn(2)−N(6)	2.043(4)	Cu(2)−N(6)	1.995(9)	Ni(2)−N(6)	1.941(7)
Zn(2)−N(7)	2.040(4)	Cu(2)−N(7)	1.992(9)	Ni(2)−N(7)	1.958(7)
Zn(2)−N(8)	2.038(4)	Cu(2)−N(8)	2.013(9)	Ni(2)−N(8)	1.971(7)

(79) Scheidt, W. R.; Lee, Y. J. *Struct. Bonding* (*Berlin*) **1987**, *64*, 1−70.
(80) Senge, M. O.; Forsyth, T. P.; Smith, K. *Z. Kristallogr*. **1996**, *211*, 176−185.

Table 4. Selected Bond Angles (deg) for **10**−**12**

10		**11**		**12**	
N(1)−Zn(1)−N(2)	89.5(2)	N(3)−Cu(1)−N(1)	176.9(3)	N(4)−Ni(1)−N(1)	90.2(3)
N(1)−Zn(1)−N(3)	172.3(2)	N(3)−Cu(1)−N(4)	88.9(4)	N(4)−Ni(1)−N(2)	179.1(3)
N(2)−Zn(1)−N(3)	91.0(2)	N(1)−Cu(1)−N(4)	90.1(4)	N(1)−Ni(1)−N(2)	89.1(3)
N(1)−Zn(1)−N(4)	90.6(2)	N(3)−Cu(1)−N(2)	91.5(3)	N(4)−Ni(1)−N(3)	89.3(3)
N(2)−Zn(1)−N(4)	178.5(2)	N(1)−Cu(1)−N(2)	89.5(3)	N(1)−Ni(1)−N(3)	178.6(3)
N(3)−Zn(1)−N(4)	88.8(2)	N(4)−Cu(1)−N(2)	178.6(3)	N(2)−Ni(1)−N(3)	91.5(3)
N(7)−Zn(2)−N(8)	89.1(2)	N(5)−Cu(2)−N(6)	89.7(4)	N(6)−Ni(2)−N(7)	91.4(3)
N(7)−Zn(2)−N(6)	91.2(2)	N(5)−Cu(2)−N(7)	175.0(3)	N(6)−Ni(2)−N(5)	88.3(3)
N(8)−Zn(2)−N(6)	175.6(2)	N(6)−Cu(2)−N(7)	91.3(4)	N(7)−Ni(2)−N(5)	178.5(3)
N(7)−Zn(2)−N(5)	172.9(2)	N(5)−Cu(2)−N(8)	90.3(4)	N(6)−Ni(2)−N(8)	177.8(3)
N(8)−Zn(2)−N(5)	90.9(2)	N(6)−Cu(2)−N(8)	179.7(3)	N(7)−Ni(2)−N(8)	88.7(3)
N(6)−Zn(2)−N(5)	88.3(2)	N(7)−Cu(2)−N(8)	88.8(4)	N(5)−Ni(2)−N(8)	91.7(3)

11. The Cu(II) ions are situated in an approximately $N_{pyrrole}$ square, as the N−Cu−N bond angles are 90 ± 1.5°. The average Cu−N bond length is 2.002 Å. A conformational analysis of the two macrocycles indicates inequivalent ring systems. The porphyrin ring containing Cu(1) exhibits a ruffled conformation with a mean deviation from planarity of 0.2176 Å; the meso carbons are alternately displaced above and below the mean porphyrin plane. In contrast, the ring with Cu(2) exhibits a wave conformation with a mean deviation from planarity of 0.3244 Å. Smith and co-workers have observed a similar effect in a related biscopper ethene-bridged bisporphyrin,[85,86] attributing this type of inequivalence to a "localized" macrocycle distortion[87,88] induced by the steric crowding of a large meso substituent flanked by proximate alkyl groups.

12. The square geometry for the Ni(II) core is confirmed by the average Ni−N_4 displacement of 0.0061 Å and N−Ni−N bond angles of 90 ± 1.7°. Deviation of Ni−N bond lengths from the 1.949 Å average (1.920(7)−1.971(7) Å) typically are caused by aggregation and packing forces.[79] The shorter M−N bond lengths in **12** as compared to **11** result from the smaller radius of the Ni(II) ion.[79,89] As observed for the analogous biscopper(II) complex **11**, the two ring systems of **12** are structurally inequivalent in the solid state. The macrocycle with Ni(1) exhibits a pronounced ruffled conformation with a mean deviation of 0.3502 Å for the macrocyclic atoms from the porphyrin mean plane. The meso carbons are alternately displaced from the mean porphyrin plane, ranging from 0.6304 Å above to 0.5829 Å below the 24-atom macrocycle unit. The S_4 ruffling of the porphyrin ring is typical of Ni(II) porphyrin complexes and results from the contraction of the metal coordination site owing to the small size and high electrophilicity of the Ni(II) ion.[90,91] The macrocycle containing Ni(2) has a less pronounced ruffled structure. Although the mean deviation of 0.3250 Å from the porphyrin plane is similar to what was observed in the ring containing Ni(1), the meso carbons are displaced from only 0.0154 Å below to 0.4076 Å above the mean porphyrin plane.

The three approximately mutually perpendicular views of the molecular crystal structures of **10**−**12** shown in Figure 4 confirm the ability of the xanthene bridge to hold two porphyrin rings in a cofacial arrangement akin to that observed for anthracene and biphenylene systems. Pertinent geometrical parameters are summarized in Table 2. Scheidt and Lee's semiquantitative scheme for the pairwise overlap of the π systems of spatially oriented porphyrin monomers within the crystalline lattice[79] provides a useful framework to analyze the structures of the xanthene bisporphyrins described here. The most important geometrical features of the aggregate dimer model are the lateral shift of the metal centers and the mean separation of the macrocycle planes, which are defined in Table 2. In this model, authentic $\pi-\pi$ interactions between aromatic macrocycles (as opposed to crystal packing effects) are signified by small lateral shifts (<4 Å).

The data of Table 2 are unique insofar as lateral shifts are collected for a homologous series of cofacial metallobisporphyrins anchored by the same pillar. Owing to the inflexibility of the xanthene spacer, the lateral shifts of **10**−**12**, defined for the most part by the methine−methine direction perpendicular to the bridge, are small and similar. Of the three structures, **12** exhibits the least π overlap, though the observed lateral shift is only moderately larger than that observed for related Ni(II) cofacial bisporphyrins (e.g., lateral shift of Ni_2(DPA) is 2.40 Å).[25] The splayed structure of **12** suggests that the association of the nickel subunits is smaller than that of the zinc and copper congeners. This finding is consonant with NMR investigations, which also show the same trend for the aggregation of monomeric, asymmetric metalloporphyrins along this metal series.[79,92−94] The interplanar mean plane separations for **10**−**12** are similar, ranging from 3.4 to 3.6 Å.

Spectroscopy. Electronic spectra of **9** and its zinc, copper, and nickel complexes are consistent with a face-to-face structure in solution. Soret (B) and Q absorption bands for **9**−**12** arising from the standard four-orbital model for porphyrin spectra[95] are clearly perturbed upon cofacially disposing two porphyrin rings. The spectrum of **10**, shown in Figure 5, is exemplary of the series. Figure 5a compares the electronic absorption spectra of

(81) Byrn, M. P.; Curtis, C. J.; Hsiou, Y.; Khan, S. I.; Sawin, P. A.; Tendick, S. K.; Terzis, A.; Strouse, C. E. *J. Am. Chem. Soc.* **1993**, *115*, 9480−9497.
(82) Osuka, A.; Nakajima, S.; Nagata, T.; Maruyama, K.; Toriumi, K. *Angew. Chem., Int. Ed. Engl.* **1991**, *30*, 582−584.
(83) Clement, T. E.; Nurco, D. J.; Smith, K. M. *Inorg. Chem.* **1998**, *37*, 1150−1160.
(84) Paolesse, R.; Pandey, R. K.; Forsyth, T. P.; Jacquinod, L.; Gerzevske, K. R.; Nurco, D. J.; Senge, M. O.; Licoccia, S.; Boschi, T.; Smith, K. M. *J. Am. Chem. Soc.* **1996**, *118*, 3869−3882.
(85) Senge, M. O.; Gerzevske, K. R.; Vicente, M. G. H.; Forsyth, T. P.; Smith, K. M. *Angew. Chem., Int. Ed. Engl.* **1993**, *32*, 750−753.
(86) Senge, M. O.; Vicente, M. G. H.; Gerzevske, K. R.; Forsyth, T. P.; Smith, K. M. *Inorg. Chem.* **1994**, *33*, 5625−5638.
(87) Hursthouse, M. B.; Neidle, S. *J. Chem. Soc., Chem. Commun.* **1972**, 449−450.
(88) Furhop, J. H.; Witte, L.; Sheldrick, W. S. *Liebigs Ann. Chem.* **1976**, 1537−1559.
(89) Fleischer, E. B.; Miller, C. K.; Webb, L. E. *J. Am. Chem. Soc.* **1964**, *86*, 2342−2347.
(90) Fleischer, E. B. *J. Am. Chem. Soc.* **1963**, *85*, 146−148.
(91) Kratzky, C.; Fassler, A.; Pfaltz, A.; Krautler, B.; Jaun, B.; Eschenmoser, A. *J. Chem. Soc., Chem. Commun.* **1984**, 1368−1371.
(92) Abraham, R. J.; Fell, S. C. M.; Pearson, H.; Smith, K. M. *Tetrahedron* **1979**, *35*, 1759−1766.
(93) Abraham, R. J.; Barnett, G. H.; Hawkes, G. E.; Smith, K. M. *Tetrahedron* **1976**, *32*, 2949−2956.
(94) Abraham, R. J.; Eivazi, F.; Pearson, H.; Smith, K. M. *J. Chem. Soc., Chem. Commun.* **1976**, 699−700.
(95) Gouterman, M. *J. Mol. Spectrosc.* **1961**, *6*, 138−163.

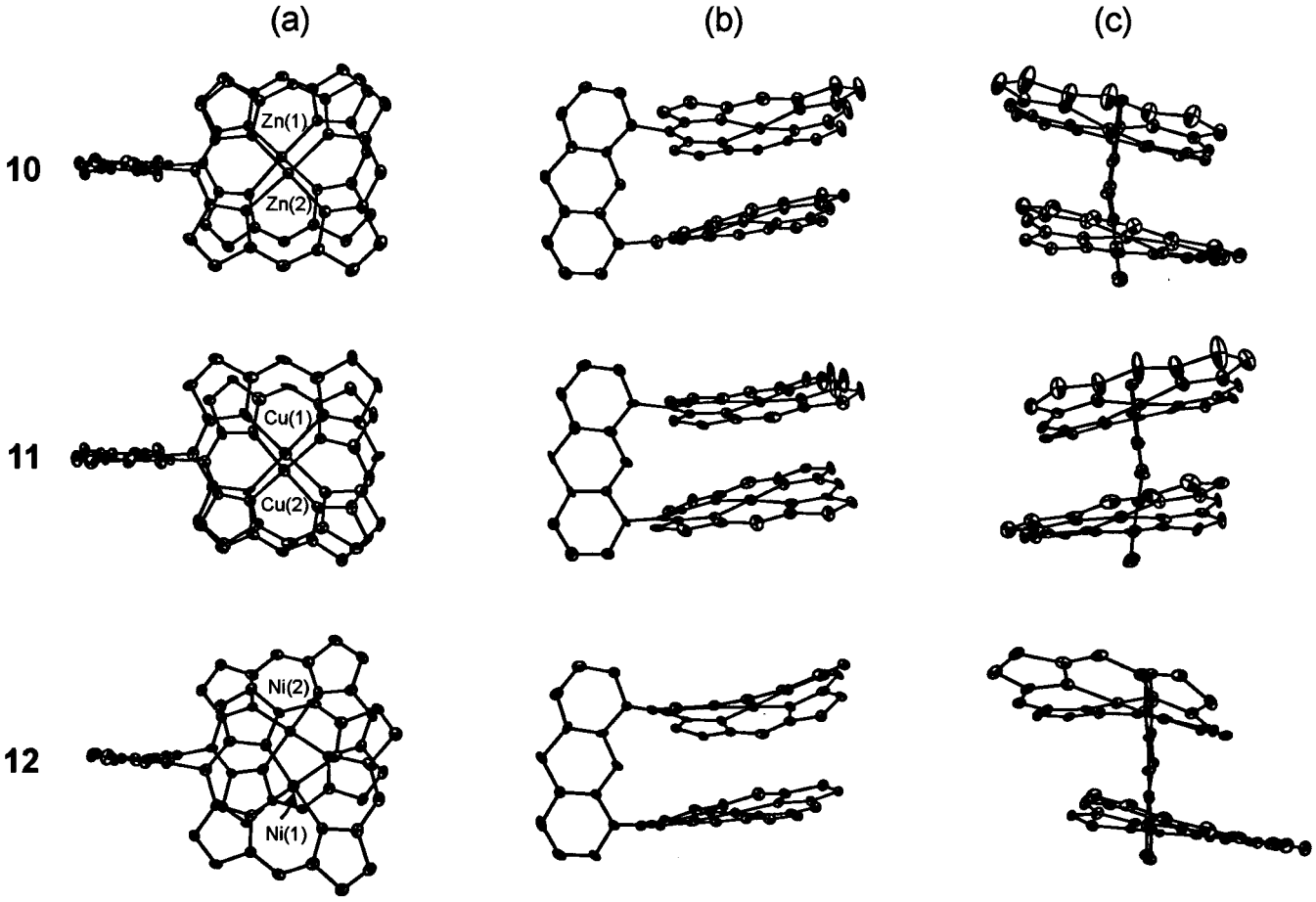

Figure 4. Comparative views of the crystal structures of **10**−**12**: (a) top view, perpendicular to porphyrin planes; (b) side view, parallel to the bridge plane; (c) side view, perpendicular to the bridge plane. Side groups have been omitted for clarity.

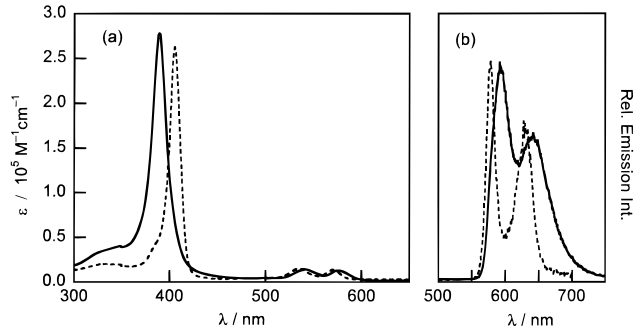

Figure 5. (a) Absorption and (b) emission spectra of Zn_2(DPX) **(10)** (solid line) and [5-(4′-bromophenyl)-2,8,13,17-tetraethyl-3,7,12,18-tetramethylporphyrinato]zinc (II) (dashed line) in dichloromethane at 298 K.

10 and its monomeric analogue [5-(4′-bromophenyl)-2,8,13,-17-tetraethyl-3,7,12,18-tetramethylporphyrinato]zinc(II) in dichloromethane. Characteristic of excitonically interacting porphyrin subunits,[4,21,22,96] the B band (λ_{max} = 389 nm, ϵ = 290 000 M^{-1} cm^{-1}) is blue-shifted and broadened relative to that of the monomer (λ_{max} = 405 nm, ϵ = 260 000 M^{-1} cm^{-1}) while Q(1,0) (λ_{max} = 541 nm, ϵ = 14 300 M^{-1} cm^{-1}) and Q(0,0) (λ_{max} = 576 nm, ϵ = 13 200 M^{-1} cm^{-1}) maxima are clearly shifted to the red (λ_{max} = 535 and 571 nm). **10** produces the strong fluorescence (τ_{obs} = 1.35(1) ns) that is typical of Q(0,0) and Q(1,0) excitation (Figure 5b). As with the Q-band absorption profile, a correspondent red shift of these emission bands (λ_{max} = 591 and 640 nm) is observed with respect to monomer emission (λ_{max} = 576 and 626 nm). Free-base porphyrin **9** also exhibits a fluorescence (λ_{max} = 637 and 703 nm, τ_{obs} = 10.55-(1) ns). The phyllo-type splitting pattern ($\lambda_{max}(Q_y(1,0))$ = 509 nm, ϵ = 10 100 M^{-1} cm^{-1}; $\lambda_{max}(Q_y(0,0))$ = 543 nm, ϵ = 5800 M^{-1} cm^{-1}; $\lambda_{max}(Q_x(1,0))$ = 579 nm, ϵ = 6200 M^{-1} cm^{-1}; λ_{max}-$(Q_x(0,0))$ = 631 nm, ϵ = 2400 M^{-1} cm^{-1}), which is characteristic of mono(meso-substituted porphyrins), though observed in the absorption profile of **9**, is not apparent in the fluorescence spectrum.

Complexes **11** and **12** exhibit typical hypso-type solution absorption spectra, due to overlap between the filled d_{xz} and d_{yz} orbitals and empty porphyrin π^* levels. The result of these interactions leads to a red shift of the porphyrin $\pi-\pi^*$ transitions with respect to those of the free-base porphyrin.[97] The B-band maximum in the absorption spectrum of **11** appears at 387 nm (ϵ = 265 000 M^{-1} cm^{-1}), with the Q(1,0) and Q(0,0) transitions occurring at 534 (ϵ = 16 700 M^{-1} cm^{-1}) and 571 nm (ϵ = 19 800 M^{-1} cm^{-1}), respectively. The B band in the absorption spectrum of **12** is centered at 388 nm (ϵ = 250 000 M^{-1} cm^{-1}). The Q bands are shifted to higher energy with respect to those of **11**, appearing at 526 nm (ϵ = 13 600 M^{-1} cm^{-1}) and 564 nm (ϵ = 23 000 M^{-1} cm^{-1}). Typical of porphyrin chemistry, the placement of the d−d states energetically below the $\pi-\pi$ states of the macrocycle circumvents luminescence.

(96) Gouterman, M.; Holten, D.; Lieberman, E. *Chem. Phys.* **1977**, *25*, 139−153.

(97) Buchler, J. W. In *Static Coordination Chemistry of Metalloporphyrins*, 2nd ed.; Smith, K. M., Ed.; Elsevier Scientific: Oxford, U.K., 1975; pp 157−232.

Concluding Remarks

The success of pillared bisporphyrins in small-molecule activation chemistry relies heavily on the choice of spacer. The most crucial features are the size and flexibility of the binding pocket provided by fixing two macrocyclic units in a cofacial arrangement. Biphenylene has been the bridge of choice in studies of the small-molecule activation chemistry of pillared bisporphyrins, providing a tighter binding cavity than the more easily synthesized anthracene due to the fewer number of atoms separating the porphyrin subunits. However, the synthesis of the biphenylene pillar is particularly arduous, involving multiple steps including a high-temperature vacuum pyrolysis (800 °C, 0.6 Torr).[29] In contrast, the accessibility of the xanthene pillar **6**, in multigram quantities in a convenient one-pot procedure without purification by column chromatography or distillation, is a noteworthy synthetic improvement over both the anthracene- and biphenylene-pillared systems. To this end, the xanthene spacer is conveniently employed in the construction of the novel pillared cofacial bisporphyrin H_4(DPX) (**9**) and the homobimetallic zinc, copper, and nickel complexes **10**−**12**, which represent the first homologous series of rigid, pillared bisporphyrins examined by X-ray diffraction.

Structural analysis confirms the ability of the xanthene bridge to hold two porphyrins in a face-to-face orientation, engendering characteristic absorption features that are indicative of exciton interactions between porphyrin chromophores. Although the xanthene bridge contains the same number of atoms as anthracene, the presence of an sp^3 oxygen in the wedge of the former gives the DPX system enhanced longitudinal flexibility, allowing the binding pocket to span the dimensions of either the anthracene or the biphenylene system. Furthermore, the pocket size of the "Pac-Man" bisporphyrin may be further tuned by metal substitution, as the extent of $\pi-\pi$ interactions plays an important role in determining the lateral slip between the two porphyrin rings. Finally, the central oxygen may provide a possible hydrogen-bonding site for proton-coupled redox processes in the bisporphyrin cavity. With these results in hand, we are now poised to investigate these and related cofacial bisporphyrin species for their small-molecule activation chemistry.

Acknowledgment. C.J.C. gratefully acknowledges the National Science Foundation for a predoctoral fellowship. We thank William Cieslik from the Hamamatsu Corp. for providing the C4334-0 streak camera, Dimitris Papoutsakis for assistance with magnetic measurements, Scott Carpenter and Al Barney for help with emission experiments, and M. Charles for providing lively discussions. This work was supported by the National Institutes of Health (Grant GM 47274).

Supporting Information Available: Tables giving complete crystallographic experimental details, bond distances and angles, positional parameters for all atoms, equivalent isotropic displacement parameters, and anisotropic displacement parameters, figures showing additional thermal ellipsoid views with full atom-labeling schemes, and X-ray crystallographic files, in CIF format, for **10**-**12**. This material is available free of charge via the Internet at http://pubs.acs.org.

IC990987+